



## Research Article

## A comparative study of three types of strength criteria for rocks

Mingming He<sup>1,\*</sup>, Qin Yang<sup>1</sup>, Panagiotis G. Asteris<sup>2</sup>, Qin Zhao<sup>1</sup><sup>1</sup> Institute of Geotechnical Engineering, Xi'an University of Technology, Xi'an 710048, China<sup>2</sup> Computational Mechanics Laboratory, School of Pedagogical and Technological Education, Heraklion, GR 14121, Athens, Greece

\* Correspondence: hemingming@xaut.edu.cn

Received: 1 September 2024  
 Revised: 26 September 2024  
 Accepted: 10 October 2024  
 Published date: 4 March 2025  
 Doi: 10.70425/rml.202501.8



Copyright: © 2024 by the authors. This is an open-access article distributed under the terms of the Creative Commons Attribution License.

**Abstract:** Currently, the unified strength criterion (USC), the three-dimensional Hoek-Brown (3D H-B) criterion and the generalized unified strength theory (GUST) are the three types of typical rock strength criteria. In this paper, a comparative study of the three types of strength criteria is performed for rocks. Based on the nonlinear characteristics of rock strength on meridian and deviatoric planes, the USC can predict rock strength under triaxial stress state. The USC is composed of two failure functions on meridian and deviatoric planes. The failure surface of the USC in principal stress space satisfies smoothness and convexity. The predicted strength for five types of rock under the true triaxial tests were compared among the USC, the GUST, and the 3D H-B criterion. The results indicate that the USC can effectively reflect the influence of the intermediate principal stress on rock strength and accurately predict rock strength under both triaxial tension ( $\sigma_1 = \sigma_2 > \sigma_3$ ) and triaxial compression ( $\sigma_1 > \sigma_2 = \sigma_3$ ). Additionally, the conventional triaxial tests were conducted on other eight types of rock to measure the strength on meridian plane. The predicted strengths for the eight types of rock on meridian plane were compared between the USC and the original H-B, which suggests that the USC is suitable for various types of rock and provides higher accuracy.

**Keywords:** Unified strength criterion; 3D H-B criterion; Generalized unified strength theory.

## 1. Introduction

Rocks are naturally complex geomaterials. Its mechanical properties are significantly influenced by stress state, lithology and other geological characteristics. Rock strength criteria can quantitatively describe the relationship among rock strength, stress state and field variables. The strength criteria guide the design of ultimate bearing capacity and safety evaluation in practical engineering and can be used to establish the constitutive relationship of rock materials. So far, many rock strength criteria have been proposed, which can be categorized [1] into the classical criteria [2-8], the modified criteria [9-23], the unified criteria [24-33].

The classical criteria include the Mohr-Coulomb criterion, the Hoke-Brown criterion [2, 3], the Lade-Duncan criterion [4, 5], the spatial mobilized plane (SMP) criterion [6-8] and etc. The Mohr-Coulomb (M-C) criterion and the Hoek-Brown (H-B) criterion are two of the most commonly used criteria for describing rock strength characteristics. Numerous researches have demonstrated that the intermediate principal stress has the notable effect on rock strength [34-45], which these two criteria fail to characterize. The Lade criterion is suitable for cohesive geomaterials, but the failure curve on deviatoric plane remains unchanged under a given internal friction angle [46]. The SMP criterion neglects the strength nonlinearity of rock on meridian plane.

Most of the modified criteria is based on the classical criteria, such as the Paul-Mohr-Coulomb criterion [9], the 3D Hoke-Brown criteria [10-22], the Zienkiewicz-Pande criterion [23]. The modification of the classical criteria for rocks has expanded its application in characterizing the strength characteristics under complex stress state. The Paul-Mohr-Coulomb criterion (P-M-C) proposed by Paul is a 3D linear strength criterion. The two sets of the P-M-C criterion can approximately delineate the nonlinear strength characteristics of rock. Many scholars have adopted the H-B criterion as the foundation for studying 3D rock strength criteria, primarily because it reflects the nonlinear strength of rock on the meridian plane. However, the current 3D H-B criteria have two main limitations. The first is that the strength criteria fail to predict the same rock strength under triaxial compression or triaxial tension as the original H-B criterion [10, 15, 17, 19, 20]. The second is that the failure surfaces of the strength criteria in the principal stress space cannot simultaneously meet smoothness and convexity requirements [12-14, 16, 18, 21, 22]. The Zienkiewicz-Pande criterion is essentially a type of modified M-C criterion, and its failure curve is quadratic on meridian plane and curvilinear on deviatoric plane. For rocks, as the hydrostatic pressure increases, the failure curve on deviatoric plane changes from a curved

triangle to a circle, which cannot be characterized by the Zienkiewicz-Pande criterion [47].

The unified strength criteria amalgamate various individual criteria. Yu et al. [24-26] proposed a unified strength theory (UST) based on the twin-shear model, which can characterize the effect of the intermediate principal stress. The UST has been widely applied in geotechnical engineering [27, 28]. However, the UST predicts the same rock strength under both triaxial tension and triaxial compression, which conflicts with the actual strength of some rocks and limits its application. By introducing a modified parameter  $\chi$  into the UST to correcting the rock strength under triaxial tension, a generalized unified strength theory (GUST) was proposed [29]. Although the GUST predicts the strength of various types of rocks more accurately, its failure surface in the principal stress space is non-smooth, leading to inconvenience of the numerical computation. Yao et al. [30, 31] proposed the unified strength criterion (USC) for geomaterials. The USC was established based on nonlinear characteristics of rock on both meridian and deviatoric planes. The stress transformation method [32, 33] was adopted for incorporating the failure functions on both meridian and deviatoric planes. Four parameters of the USC control the shape of failure curve, which can effectively characterize the shape transition of the failure curve from a curved triangle to a circle. Liu et al. [48] proposed a 3D nonlinear strength criterion (3D NSC) for rocks by combining the segmented meridian function and the generalized deviatoric function with one parameter. The 3D NSC can accurately describe and predict the strength change of rock in both brittle and ductile domains.

The rock criteria can be categorized into the linear strength theory and the nonlinear strength theory [27]. A criterion can be classified as the linear strength theory only if the failure curves are linear on both meridian and deviatoric planes, whereas if the failure curve is nonlinear on either meridian plane or deviatoric plane, it is classified as the nonlinear strength theory. The linear strength theory includes the M-C criterion, the twin shear stress theory [24]. The nonlinear strength theory includes the Hoek-Brown (H-B) criterion [2, 3], the SMP criterion [6-8], the Lade criterion [4, 5]. The failure curves of the M-C criterion and the twin-shear theory are linear on the two planes. The failure curve of H-B criterion is parabolic on meridian plane and linear on deviatoric plane, respectively. The SMP criterion appears as a linear function on meridian plane, and curvilinear shape on deviatoric plane. The Lade criterion has a linear relationship on meridian plane and a curvilinear relationship on deviatoric plane. The Zienkiewicz-Pande criterion presents failure curve with quadratic forms on meridian plane and the curvilinear form on deviatoric plane.

The strength test methods for rocks under different stress conditions mainly include the conventional triaxial test (CTT) and true triaxial test (TTT). The CTT was perhaps first conducted by Karman under the stress state that the intermediate and minimum principal stresses are equal [49]. Due to the simplicity of the equipment and ease of sample preparation, the CTT has been widely applied in rock mechanics experiments [50-53]. The CCT is suitable for testing the strength of a type of rock with the weak intermediate principal stress effect. The TTT apparatus designed by Mogi may first enable the application of three mutually independent and uniform loads to the specimen faces [54]. The TTT conducted by Mogi found that the maximum principal stress  $\sigma_1$  at failure is a function of  $\sigma_2$  with concave curve of  $\sigma_1$  vs.  $\sigma_2$  under constant  $\sigma_3$ . The theories and applications based on the TTT have been verified by practical engineering cases such as coal mining [55], wellbore stability [56] and rock-burst [57, 58]. Therefore, both of the CTT and TTT are the effective methods for measuring rock strength. In particular, the TTT can measure the rock strength under more complex stress state.

In summary, a versatile rock strength criterion needs to meet the following functions: (i) the influence of the intermediate principal stress on rock strength is effectively characterized; (ii) the failure surface of the strength criterion in the principal stress space is smooth and convex; (iii) the parameters of the strength criterion have clear physical meanings; (iv) the criterion can be conveniently integrated with elastoplastic constitutive models. To determine the advantages and disadvantages of the rock strength criteria, three types of rock strength criteria were compared in this paper. These rock strength criteria are the USC [31], the GUST [29] and 3D H-B [20]. By comparing the USC with the GUST and the 3D H-B, the advantages of the USC are determined. Finally, based on the conventional triaxial test results for eight types of rock, the accuracy of rock strength predicted by the original H-B criterion and the USC was compared.

## 2. Three typical rock strength criteria

### 2.1. 3D H-B criterion

Based on Griffith's strength theory and combined with a large amount of triaxial test for rocks, the original H-B criterion was first proposed by Hoek and Brown in 1980 [3]. It can be expressed as

$$\sigma_1 = \sigma_3 + \sigma_c \left( m_i \frac{\sigma_3}{\sigma_c} + 1 \right)^{0.5} \quad (1)$$

where  $\sigma_1$  is the maximum principal stress;  $\sigma_3$  is the minimum principal stress;  $\sigma_c$  is the uniaxial compressive strength of rock;  $m_i$  is a constant reflecting the degree of softness and hardness of rock, which ranges from 0.001 to 25.0. The failure curve of the H-B strength criterion in meridian plane is parabolic. It can be expressed as

$$\begin{cases} q = -\frac{m_i \sigma_c}{6} + \sqrt{m_i \sigma_c p + \frac{m_i^2 \sigma_c^2}{36} + \sigma_c^2} \\ p = \frac{1}{3(\sigma_1 + \sigma_2 + \sigma_3)} \\ q = \frac{\sqrt{2}}{2[(\sigma_1 - \sigma_2)^2 + (\sigma_2 - \sigma_3)^2 + (\sigma_3 - \sigma_1)^2]} \end{cases} \quad (2)$$

where  $p$  is the hydrostatic pressure;  $q$  is the generalized shear stress.

Based on the SMP criterion and the Drucker-Prager (D-P) criterion, Du et al. [59] developed the nonlinear unified strength theory (NUST). A new stress space,  $\beta$  stress space, is adopted in the NUST. On deviatoric plane, the NUST can be expressed as,

$$p_\beta = \sigma_1^\beta + \sigma_2^\beta + \sigma_3^\beta = p_{\beta 0} \quad (3)$$

where  $p_\beta$  is the hydrostatic pressure in  $\beta$  stress space, and  $p_{\beta 0}$  is the initial value of  $p_\beta$ ;  $\sigma_i^\beta$  ( $i=1,2,3$ ) is the principal stress in  $\beta$  stress space.

Considering the effect of the intermediate principal stress, Huang et al. [20] integrated the NUST with the H-B criterion by the stress-space transformation method. Therefore, the 3D H-B criterion applicable to describing strength characteristics of rock under triaxial stress state was established. The 3D H-B criterion is defined as,

$$\begin{cases} q_\beta = m_t \left( -\frac{m_i \sigma_c}{6} + \sqrt{m_i \sigma_c p + \frac{m_i^2 \sigma_c^2}{36} + \sigma_c^2} \right) \\ q_\beta = M_\beta p_\beta \end{cases} \quad (4)$$

where  $M_f$  is a material parameter;  $M_\beta$  is the failure stress ratio;  $m_t$  is the ratio of the triaxial tension strength and the triaxial compression strength under the same hydrostatic stress and calculated by  $M_\beta$ ,  $M_f$  and  $\beta$ .

The 3D H-B criterion constructs the strength curves on meridian and deviatoric planes based on the H-B criterion and the NUST, respectively. By employing a stress-space transformation method, it combines the strength curves on meridian and deviatoric planes, thereby establishing a new 3D rock strength criterion.

### 2.2. Generalized unified strength theory

Yu and He proposed a unified strength theory (UST) based on a twin-shear model [26]. It can be expressed as follows:

$$\text{when } \tau_{12} + \beta \sigma_{12} \geq \tau_{12} + \beta \sigma_{23}$$

$$F = \tau_{12} + b\tau_{12} + \beta(\sigma_{13} + b\sigma_{12}) = C \quad (5a)$$

$$\text{when } \tau_{12} + \beta \sigma_{12} \leq \tau_{12} + \beta \sigma_{23}$$

$$F = \tau_{13} + b\tau_{23} + \beta(\sigma_{13} + b\sigma_{23}) = C \quad (5b)$$

where  $b$  is a parameter reflecting the influence of  $\tau_{12}$  and  $\tau_{23}$  on the failure of materials;  $\beta$  is the coefficient reflecting the effect of normal stresses on failure;  $C$  is a material constant. The values of  $\beta$  and  $C$  can be determined by uniaxial tension strength  $\sigma_t$  and uniaxial compression strength  $\sigma_c$  respectively.

The UST can be expressed by the principal stresses as follows:

$$\text{when } \sigma_2 \leq (\sigma_1 + a\sigma_3)/(1 + a)$$

$$F = \sigma_1 - \frac{a}{1+b} (b\sigma_2 + \sigma_3) = \sigma_t \quad (6a)$$

$$\text{when } \sigma_2 \geq (\sigma_1 + a\sigma_3)/(1 + a)$$

$$F = \frac{1}{1+b} (\sigma_1 + b\sigma_2) - a\sigma_3 = \sigma_t \quad (6b)$$

where  $a = \sigma_t / \sigma_c$ . The UST expressed by the principal stresses from Eq. 6 incorporate the intermediate principal stress  $\sigma_2$ , which implies that the strength characteristics of the rock can be characterized more accurately.

Rock strength predicted by the UST are equal under triaxial compression and triaxial tension, which limits its application. Li et al. [29] modified the UST by introducing a parameter  $\chi$  and proposed the generalized unified strength theory (GUST). The expression of the GUST is as follows:

$$\text{when } \sigma_2 \geq \sigma_2^*$$

$$F = \frac{\sigma_1 + \chi b \sigma_2}{1+b} - \frac{1 + \sin \varphi}{1 - \sin \varphi} \sigma_3 = \frac{2c \cos \varphi}{1 - \sin \varphi} \quad (7a)$$

$$\text{when } \sigma_2 \leq \sigma_2^*$$

$$F = \sigma_1 - \frac{b \sigma_2 + \sigma_3}{1+b} \frac{1 + \sin \varphi}{1 - \sin \varphi} = \frac{2c \cos \varphi}{1 - \sin \varphi} \quad (7b)$$

where  $\sigma_2^*$  is the turning point of the  $\sigma_2^*$  effect corresponding to the maximum strength,  $\sigma_2^* = \sigma_1 [(1 - \sin \varphi) + \sigma_3 (1 - \sin \varphi)] / [(1 + \chi) + (1 - \chi) \sin \varphi]$ ; the factor  $\chi$  characterizes the mobilization of the weakening effect of  $\sigma_2$  when  $\sigma_2 \geq \sigma_2^*$ , and it can be determined from the conventional triaxial tension test,

$$\chi = \frac{2(\sin \varphi - \sin \varphi_e)}{b(1 - \sin \varphi)(1 + \sin \varphi_e)} + \frac{(1 + \sin \varphi)(1 - \sin \varphi_e)}{(1 - \sin \varphi)(1 + \sin \varphi_e)} \quad (8a)$$

or

$$\frac{1 + \chi b}{1+b} = \frac{(1 + \sin \varphi)(1 - \sin \varphi_e)}{(1 - \sin \varphi)(1 + \sin \varphi_e)} \quad (8b)$$

where  $\varphi_e$  is the friction angle under triaxial tension. As explained above, the strength characteristics depends on the mobilization of  $\sigma_2$ -effect in the complex stress state. The GUST is based on the twin-shear model. It introduces the parameter  $\chi$ , which enables the twin-shear model to be applied to some types of rock with higher triaxial tensile strength than triaxial compressive strength.

### 2.3. Unified strength criterion

Based on experimental law, the rock strength exhibited nonlinear behavior both on deviatoric plane and meridian plane [30]. The USC was proposed for characterizing the nonlinear behavior of the rock strength. On deviatoric plane, the USC unifies the SMP criterion and the Mises criterion by linear interpolation.

1. The failure curve of the Mises criterion on  $\pi$ -plane in original stress space can be expressed as follows:

$$q_M^* = \sqrt{I_1^2 - 3I_2} \tag{9}$$

2. The failure curve of the SMP criterion on  $\pi$ -plane in original stress space can be expressed as follows:

$$q_S^* = \frac{2I_1}{3\sqrt{(I_1I_2 - I_3)/(I_1I_2 - 9I_3)} - 1} \tag{10}$$

where  $q^*$  is deviator stress;  $I_1, I_2$  and  $I_3$  represent the first, second and third stress invariant, respectively;

A linear interpolation of the SMP criterion and the Mises criterion is conducted by introducing a material parameter  $\alpha$ . The expression of the USC can be expressed as follows:

$$q_\alpha^* = \alpha q_M^* + (1 - \alpha)q_S^* \tag{11}$$

As shown in Fig. 1,  $\alpha$  is a factor controlling the shape of the USC on  $\pi$ -plane.  $\alpha$  varies within the range of 0 to 1.  $\alpha=0$  and  $\alpha=1$  represent the SMP criterion and the Mises criterion respectively. Therefore, the shape of the USC on deviatoric plane can transmit from a curved triangle to a circle with  $\alpha$  increasing.

On meridian plane, a failure function of the USC can be established as a power function [30],

$$q_\alpha^* = M_f \left( \frac{p + \sigma_0}{p_r} \right)^n p_r \tag{12}$$

where  $p$  is mean stress;  $p_r$  is given reference pressure;  $M_f$  and  $n$  are material parameters;  $\sigma_0$  is triaxial tension strength.

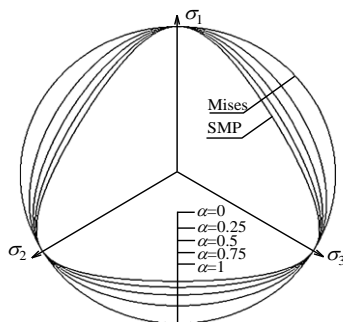


Fig. 1. Failure curve on  $\pi$ -plane [31].

Notice that if establishing the strength criterion by combining the failure functions on deviatoric and meridian planes, one of the two points should be satisfied at least: (i) the failure function on meridian plane is linear; (ii) the failure curve on deviatoric plane is circular. The failure curves of the USC on deviatoric and meridian planes are a curve triangle and nonlinear respectively. Thus, a transformed method is adopted for the failure function on meridian plane of the USC, which can transform the nonlinear failure curve into the linear failure curve. The failure curves on deviatoric planes in original and transition spaces are shown in Figure 2. The failure curve passes a fixed point  $(p_r, M_f p_r)$ . Transformation relationship is defined as,

$$\begin{cases} \bar{q}_\alpha^* = M_f \bar{p} \\ \bar{p} = \left( \frac{p + \sigma_0}{p_r} \right)^n p_r \end{cases} \tag{13}$$

where  $\bar{p}$  is mean stress in transformed stress space.

The stress tensor in transition space is expressed as,

$$\begin{cases} \bar{I}_1 = \bar{\sigma}_1 + \bar{\sigma}_2 + \bar{\sigma}_3 \\ \bar{I}_2 = \bar{\sigma}_1 \bar{\sigma}_2 + \bar{\sigma}_2 \bar{\sigma}_3 + \bar{\sigma}_3 \bar{\sigma}_1 \\ \bar{I}_3 = \bar{\sigma}_1 \bar{\sigma}_2 \bar{\sigma}_3 \end{cases} \tag{14}$$

$$\bar{\sigma}_i = \sigma_i + \left[ \left( \frac{p + \sigma_0}{p_r} \right)^n p_r - p \right] \tag{15}$$

where  $\bar{\sigma}_i$  ( $i=1,2,3$ ) represents the principal stress in transformed stress space. In transformed stress space, the new unified strength criterion, the USC, satisfies a condition that is the linear failure function on meridian

plane. Therefore, the USC can be established by combing the failure functions on deviatoric and meridian planes ( $\bar{\sigma}_3 > 0$ ),

$$\begin{cases} \bar{q}_\alpha^* = M_f \left( \frac{\bar{p}}{p_r} \right)^n p_r \\ \bar{q}_\alpha^* = \alpha \sqrt{I_1^2 - 3I_2} + \frac{(1 - \alpha)2I_1}{3\sqrt{(I_1I_2 - I_3)/(I_1I_2 - 9I_3)} - 1} \end{cases} \tag{16}$$

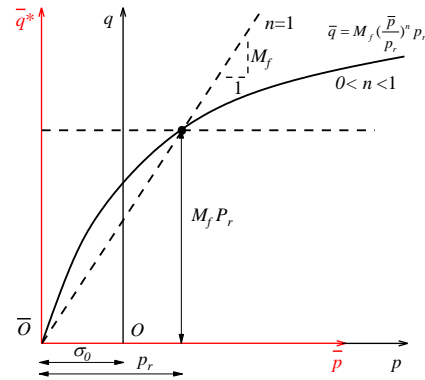


Fig. 2. Failure curve on meridian plane [31].

The USC constructs the strength curve on meridian and deviatoric planes based on the empirical power function and a linear combination of the SMP and Mises criteria, respectively. It also combines the strength curves on these two planes by using a stress-space transformation method.

### 3. Rock strength test

#### 3.1. True triaxial test

The true triaxial test results are quoted from the references [37-39]. The USC was verified by the true triaxial test from five types of rock including Dunham dolomite [37], KTB amphibolite [39], Shirahama sandstone [38], Solnhofen limestone [37] and Yuubari shale [38]. The true triaxial tests were conducted under different  $\sigma_3$  levels. The tests data are shown in Table 1-5.

#### 3.2. Conventional triaxial test

##### 3.2.1. Test equipment

The conventional triaxial tests were conducted on WDT-1500 Rock Test System with an axial load capacity of 1500 kN, confining pressure capacity of 80 MPa (see Fig. 3). The WDT-1500 controller consists of a hardware component and software applications. It includes four main parts: a digital servo controller, an axial dynamic loading system, a self-balanced pressure chamber and a data acquisition system. The computer is used to control the host to run the experiment.

##### 3.2.1. Test Specimen

Eight types of rock, green sandstone, tuff, mudstone, fine sandstone, cyan sandstone, granite, grey sandstone and micritic limestone are selected to test strength in this paper. The rock samples were obtained from the surrounding rock of a tunnel in Qinlin Mountain, Shaanxi Province, China. The samples were cut into standard cylinders 50 mm in diameter and 100 mm in length according to the ISRM testing procedure and guidelines.



Fig. 3. WDT-1500 Rock Testing System.

**Table 1.** Summary of true triaxial compression tests of Dunham dolomite.

$\sigma_1$ (MPa)	$\sigma_2$ (MPa)	$\sigma_3$ (MPa)
400	25	25
475	66	25
495	96	25
560	129	25
571	174	25
586	229	25
545	272	25
487	45	45
570	97	45
576	126	45
606	160	45
639	183	45
670	240	45
670	266	45
622	294	45
540	60	60
568	65	65
638	117	65
644	153	65
687	208	65
685	262	65
746	318	65
701	393	65
620	85	85
684	128	85
719	153	85
744	233	85
773	306	85
818	376	85
798	445	85
682	105	105
778	167	105
786	205	105
805	268	105
863	270	105
824	334	105
840	356	105
822	415	105
725	125	125
824	187	125
860	239	125
863	293	125
897	362	125
941	414	125
918	463	125
886	516	125

**Table 2.** Summary of true triaxial compression tests of KTB amphibolite.

$\sigma_1$ (MPa)	$\sigma_2$ (MPa)	$\sigma_3$ (MPa)
176	0	0
346	80	0
291	150	0
347	200	0
267	230	0
410	30	30
479	60	30
599	100	30
652	200	30
571	250	30
637	300	30
702	60	60
750	90	60
766	100	60
745	155	60
816	200	60
888	250	60
828	300	60
887	350	60
954	400	60
815	450	60
868	100	100
959	160	100

1001	200	100
945	250	100
892	270	100
1048	300	100
1058	350	100
1155	440	100
1118	600	100
1147	150	150
1065	200	150
1112	200	150
1176	250	150
1431	300	150
1326	350	150
1169	400	150
1284	450	150
1265	500	150
1262	640	150

**Table 3.** Summary of true triaxial compression tests of Shirahama sandstone.

$\sigma_1$ (MPa)	$\sigma_2$ (MPa)	$\sigma_3$ (MPa)
98	9	5
100	15	5
89	29	5
111	46	5
95	64	5
113	15	8
133	27	8
136	41	8
138	52	8
129	74	8
161	30	15
167	61	15
167	82	15
164	88	15
172	98	15
184	30	20
174	42	20
188	52	20
186	61	20
198	73	20
197	85	20
195	100	20
187	104	20
223	50	30
228	73	30
234	93	30
231	113	30
243	133	30
226	153	30
217	174	30
245	61	40
256	73	40
260	83	40
256	103	40
276	103	40
268	124	40
284	143	40
277	164	40

3.2.3. Test method

Uniaxial compression strength tests and conventional triaxial tests were conducted on each type of rock. During the tests, a constant confining pressure was applied to the rock samples, and the axial pressure was gradually increased until the rock failed. The loading rate of axial force was set at 0.1 kN/s. The confining pressures applied to green sandstone and tuff were 2, 7, 10, and 13 MPa, and 4, 8, 12, and 16 MPa, respectively. For the rest rock samples, the confining pressures were 5, 10, 15, and 20 MPa. The test results were summarized in Table 6.

4. Comparison among the USC, the GUST and 3D H-B criterion

All parameters of the USC are shown in Figure 4. The results of true triaxial tests illustrate the strength variation of five types of rock from triaxial compression to triaxial tension. From Figure 4, the following

conclusions can be drawn: (1)  $\sigma_2$  significantly affects rock strength; (2)  $\sigma_2$  effect on rock strength exhibits an interval pattern, which refers that as  $\sigma_2$  increases from the lower limit value ( $\sigma_2=\sigma_3$ ) to the upper limit value ( $\sigma_1=\sigma_2$ ), rock strength initially increases, then decreases once  $\sigma_2$  reaches a certain value; (3) rock strength increases as  $\sigma_3$  increases; (4) rock strength under triaxial tension is slightly greater than that under triaxial compression. (5) the degree of  $\sigma_2$  effect of Yuubari shale and Shirahama sandstone is smaller than other types of rock, which means the degree of  $\sigma_2$  effect varies among different types of rock.

**Table 4.** Summary of true triaxial compression tests of Solnhofen limestone.

$\sigma_1$ (MPa)	$\sigma_2$ (MPa)	$\sigma_3$ (MPa)
397	20	20
417	51	20
413	92	20
453	165	20
460	206	20
465	233	20
449	40	40
446	40	40
486	80	40
499	113	40
530	193	40
547	274	40
535	315	40
517	87	60
537	102	60
530	113	60
576	164	60
550	197	60
553	275	60
557	345	60
528	80	80
572	126	80
577	150	80
647	208	80
591	225	80
677	283	80
665	298	80
650	378	80
680	454	80

**Table 5.** Summary of true triaxial compression tests of Yuubari shale.

$\sigma_1$ (MPa)	$\sigma_2$ (MPa)	$\sigma_3$ (MPa)
160	25	25
167	25	25
181	36	25
187	36	25
175	45	25
175	57	25
186	66	25
200	77	25
194	79	25
196	86	25
200	96	25
194	101	25
185	115	25
197	125	25
183	134	25
236	49	50
256	70	50
259	91	50
265	100	50
258	110	50
258	123	50
285	130	50
265	149	50
256	160	50

The 3D H-B criterion and USC describe the strength characteristics of rock in a nonlinear form, while GUST describe those in a piecewise linear form. For Dunham dolomite (see Fig. 4a),  $\sigma_3$  ranges from 25 to 125 MPa with a constant interval of 20 MPa. The value of  $\sigma_2$  corresponding to the

maximum strength predicted by the USC is greater than that predicted by the other two criteria, for example, when  $\sigma_3=125$  MPa,  $\sigma_2^{USC}=550$  MPa,  $\sigma_2^{3D\ H-B}=426$  MPa,  $\sigma_2^{GUST}=370$  MPa. The maximum increase ratio of rock strength from triaxial compression to triaxial tension predicted by the USC, the GUST, and the 3D H-B criterion is 34.01%, 17.31%, and 14.42%, respectively.

For KTB amphibolite,  $\sigma_3$  ranges from 0 to 150 MPa with intervals of 30 MPa, 40 MPa, and 50 MPa (see Fig. 4b). The length of the strength increase section predicted by the USC is still greater than that of the other two criteria. Among the three criteria, the rock strength predicted by the 3D H-B under triaxial tension is lower than that under triaxial compression when  $\sigma_3$  is greater than 0 MPa, while the other criteria maintain the prediction that the triaxial tension strength is greater than the triaxial compression strength. The 3D H-B criterion shows a significant drop in rock strength after reaching the maximum value when  $\sigma_3$  is greater than 30 MPa, resulting in an obvious error. Compared with other criteria, the rock strength predicted by the USC and the actual values have good fitting results.

For Shirahama sandstone,  $\sigma_3$  ranges from 8 to 40 MPa with intervals of 5 MPa, 7 MPa, and 10 MPa (see Fig. 4c). When the values of are 8 MPa, 15 MPa, and 20 MPa, the rock strength predicted by the USC criterion is lower than the actual values near triaxial compression. When the values of  $\sigma_3$  are 30 MPa and 40 MPa, the rock strength predicted the 3D H-B criterion is significantly lower than the actual values near the triaxial tension state. The errors between the rock strength predicted by the GUST and the actual values are not obvious. For Solnhofen limestone and Yuubari shale, none of the three criteria shows significant errors in fitting rock strength (see Fig. 4d, e).

**Table 6.** Summary of conventional triaxial compression tests of eight types of rock.

Rock type	$\sigma_1$ (MPa)	$\sigma_2=\sigma_3$ (MPa)	$p$ (MPa)	$q$ (MPa)	$\sigma_c$ (MPa)
Green sandstone	69.00	2	24.33	67.00	60
	94.75	7	36.25	87.75	
	123.30	10	47.77	113.30	
	169.00	13	65.00	156.00	
Tuff	92.50	4	33.50	88.50	70
	141.00	8	52.33	133.00	
	157.00	12	60.33	145.00	
	169.00	16	67.00	153.00	
Mudstone	36.80	5	15.60	31.80	25
	66.20	10	28.73	56.20	
	71.40	15	33.80	56.40	
	103.00	20	47.67	83.00	
Fine sandstone	50.07	5	20.02	45.07	42
	60.42	10	26.81	50.42	
	68.56	15	32.85	53.56	
	75.01	20	38.34	55.01	
Cyan sandstone	84.22	5	31.41	79.22	67
	90.66	10	36.89	80.66	
	106.70	15	45.57	91.70	
	125.22	20	55.07	105.22	
Granite	95.46	5	35.15	90.46	78
	105.88	10	41.96	95.88	
	117.01	15	49.00	102.01	
	140.13	20	60.04	120.13	
Grey sandstone	90.40	5	33.47	85.40	75
	95.80	10	38.60	85.80	
	103.00	15	44.33	88.00	
	128.30	20	56.10	108.30	
Micritic limestone	154.88	10	58.34	144.82	90
	197.87	25	82.68	172.80	
	281.45	40	120.56	241.34	
	157.24	10	59.12	147.18	
	265.52	25	105.25	240.41	
	288.16	40	122.82	248.00	

In order to compare the USC with other strength criterions quantitatively, the root-mean-square error (RMSE, MPa) between the predicted strength and the tested data is defined as,

$$RMSE = \sqrt{\frac{\sum_{i=1}^n (\sigma_{1i}^{calc} - \sigma_{1i}^{test})^2}{n}} \tag{17}$$

where the unit of RMSE is MPa;  $\sigma_{li}^{test}$  and  $\sigma_{li}^{calc}$  are tested data and calculated data of  $i$ -th the first principal stress respectively;  $n$  is the total number of test samples.

As shown in Figure 5, the RMSE ranges for the USC, the 3D H-B criterion, and the GUST are 7.35 MPa to 69.12 MPa, 8.74 MPa to 108.32 MPa, and 8.63 MPa to 109.12 MPa respectively, which indicate that USC is the optimal criterion in predicting rock strength. It is known that the effect of  $\sigma_2$  on rock strength can be divided into two parts: a strengthening region at low  $\sigma_2$  values, and a weakening region at high  $\sigma_2$  values. In addition, the triaxial tension strength of rock is slightly greater than the triaxial compression strength.

The USC accurately characterizes the effect of  $\sigma_2$  due to integration of the nonlinear characteristics of rock strength both on deviatoric plane and meridian plane. The GUST characterizes the effect of  $\sigma_2$  by introducing the parameter  $b$ , and adjusts the fitting results by introducing the mobilized parameter  $\chi$  to make the triaxial tension strength of the rock greater than the triaxial compression strength. For the 3D H-B criterion, when the stress state of rock is approaching triaxial tension state, the errors between fitting values and actual values become more significant, particularly in KTB amphibolite. The deficiency of 3D H-B criterion is mainly related to the overestimation of the weakening effect at high  $\sigma_2$  values.

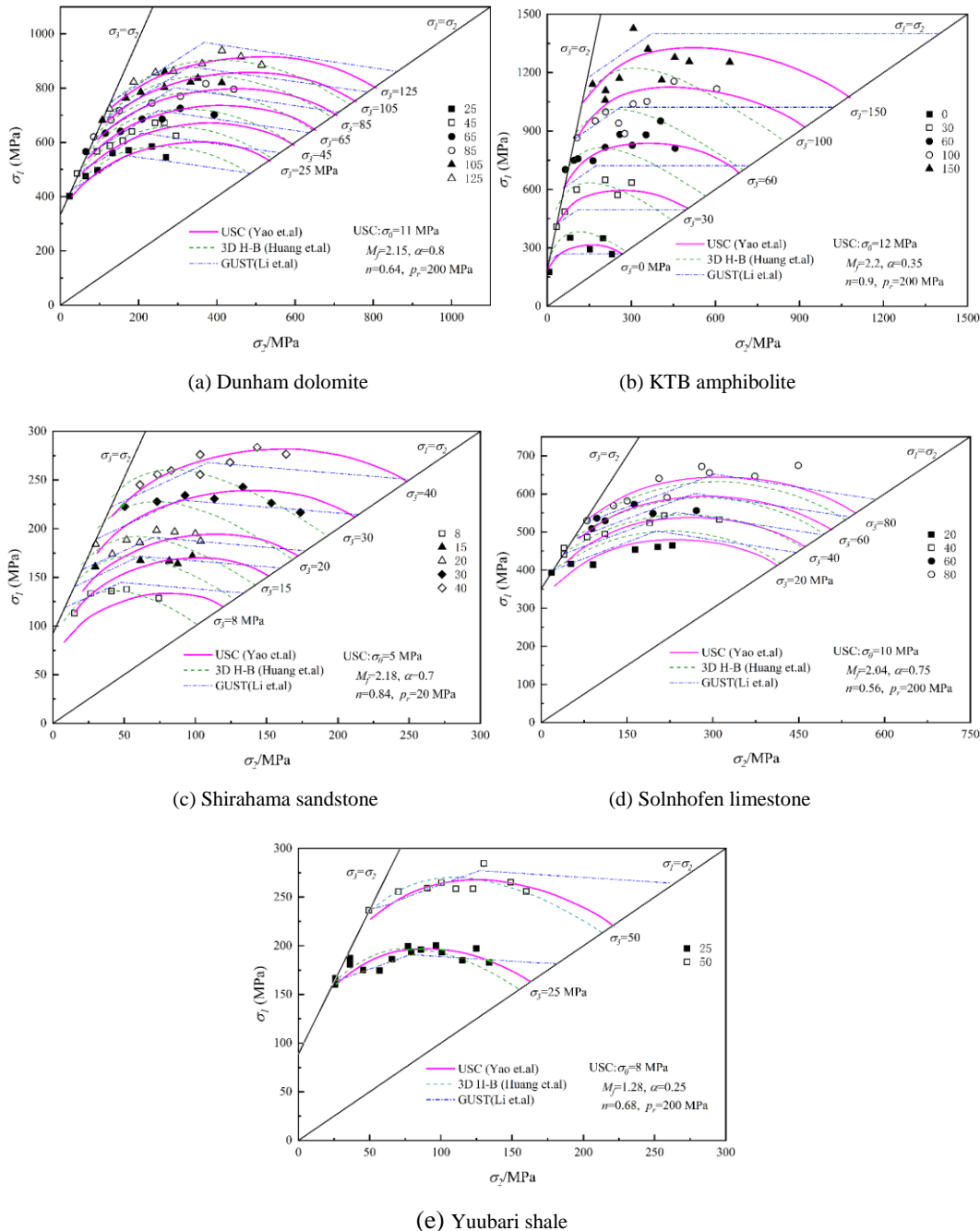


Fig. 4. Comparisons among the USC, the GUST and 3D H-B criterion  $\sigma_2$ - $\sigma_1$  plane.

5. Rock strength predicted by USC on meridian plane

To further validate the applicability of the USC for different types of rock, the conventional triaxial tests were conducted on eight types of rock, including green sandstone, tuff, mudstone, fine sandstone, cyan sandstone, granite, grey sandstone and micritic limestone.  $M_f, n, \sigma_0$  and  $p_r$  were determined by the methods provided in reference [31].

The test results show that the deviatoric stress  $q$  increases monotonically with an increase of the hydrostatic pressure  $p$  (see Fig.6). The failure curve fitted by the USC on meridian plane includes linear and

nonlinear forms, which are controlled by the parameter  $n$ . The failure curve fitted by the original H-B criterion only has a nonlinear form. The intersection of the failure curve of rock on meridian plane with the  $p$ -axis represents the true triaxial tensile strength. In the USC, the true triaxial tensile strength of the rock can be evaluated directly [31], whereas the original H-B criterion cannot provide the reasonable true triaxial tensile strength. For example, the true triaxial tensile strength of Fine sandstone calculated by the USC criterion is -3.97 MPa, while the true triaxial tensile

strength of Fine sandstone calculated by the original H-B criterion is - 26.36 MPa, which is 6.64 times than that calculated by the USC.

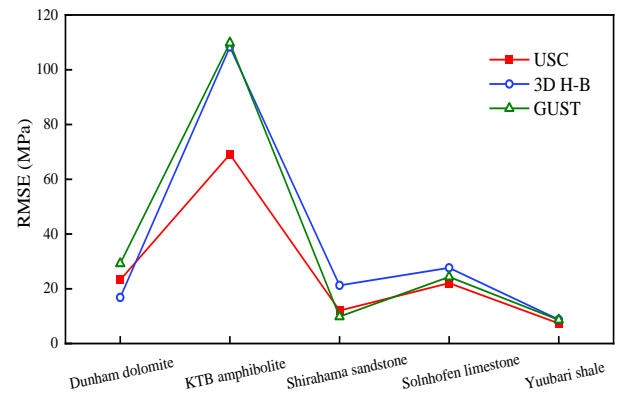
The RMSE of  $q$  for the USC and the original H-B criterion has been calculated according to Eq. (21). Figure 7 shows the RMSE of  $q$  for all types of rock. The RMSE of  $q$  for the USC and the original H-B criterion ranges from 0.69 MPa to 4.9 MPa and 0.72 MPa to 7.88 MPa respectively. The RMSE interval of  $q$  for the USC falls within that of the original H-B criterion, which suggests that the USC can predict the different types of rock more accurately than the original H-B criterion. On the other hand, the USC overcomes the shortcoming of some 3D H-B criteria, which cannot predict the same rock strength as the H-B criterion [10, 15, 17, 19, 20].

**6. Discussion**

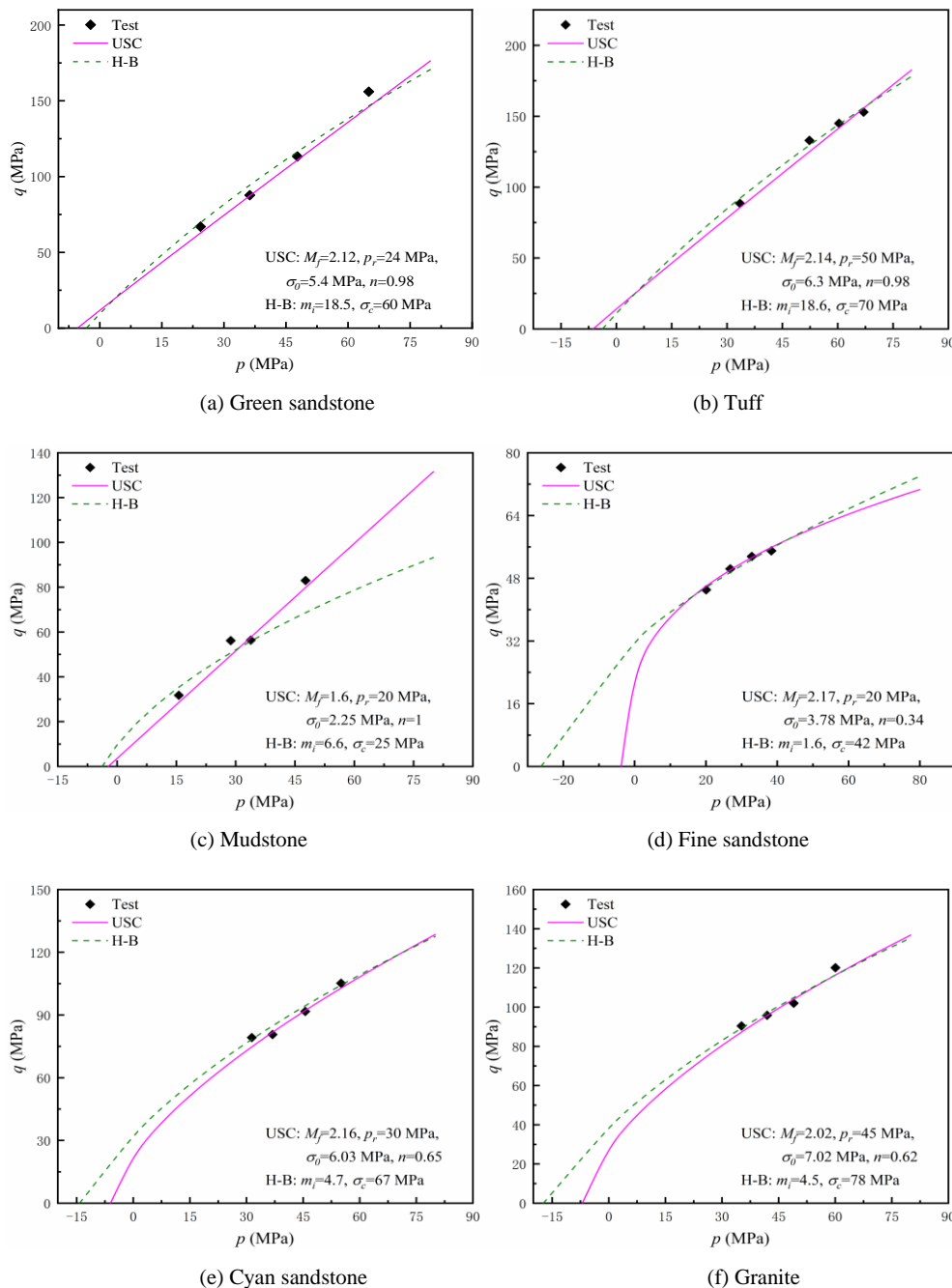
The GUST, the 3D H-B criterion, and the USC all belong to the unified strength theory. Each of the three criteria can be degenerated into a single strength criterion by changing values of the relevant parameters.

When  $b=0$ , the GUST reduces to the Mohr-Coulomb criterion. When  $b=1/2$  and  $(1-\sin\varphi)/(1+\sin\varphi)=0$ , the GUST becomes the linear approximation of the Mises criterion. When  $b=0$  and  $(1-\sin\varphi)/(1+\sin\varphi)=1$ , the GUST becomes the Tresca criterion. For the 3D H-B criterion, when

$m_i=1$ , it reduces to the original H-B criterion; it becomes the SMP criterion with  $\beta=0$  and Drucker-Prager criterion with  $\beta=1$ . For the USC criterion, it reduces to the SMP criterion with  $\alpha=0$  and the Mises criterion with  $\alpha=1$ .



**Fig. 5.** RMSE of  $\sigma_1$  from the USC, the 3D H-B and the GUST.



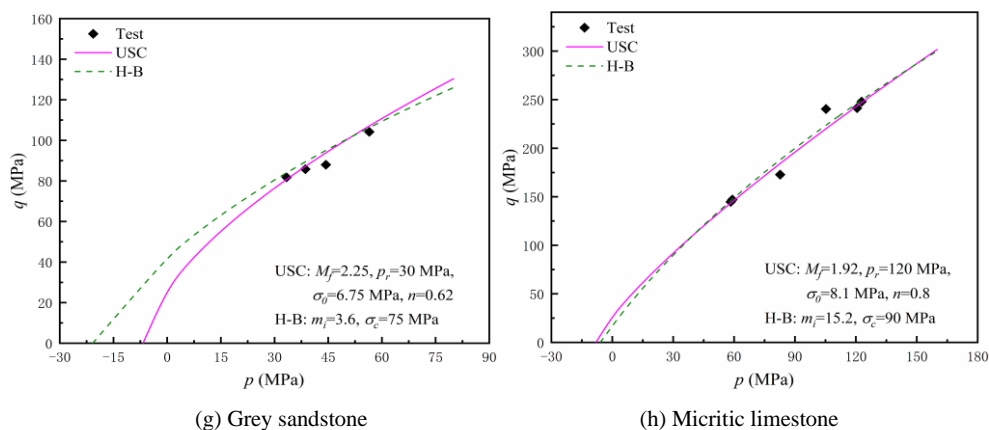


Fig. 6. Comparisons between the USC and the original H-B criterion.

The parameters of the three criteria are determined through the true triaxial tests or conventional triaxial tests. The GUST includes four parameters  $c, \varphi, \chi$  and  $b$ .  $c$  and  $\varphi$  can be determined by conventional triaxial tests.  $b$  and  $\chi$  can be determined jointly using the least square method based on the results of true triaxial tests [29]. The 3D H-B criterion includes six parameters  $\sigma_c, m_i, m_t, M_\beta, M_f$  and  $\beta$ . These six parameters are not mutually independent. As long as  $m_t$  is determined, the  $M_\beta, M_f$  and  $\beta$  will be determined. In general,  $m_t$  is determined by true triaxial tests. When some types of rock satisfy the negative exponential empirical relationship between  $m_i$  and  $m_t, m_t = [(m_i + 1)^{-0.371} + 1] / 2$ , the five parameters of the 3D H-B can be reduced to two parameters  $\sigma_c$  and  $m_i$  [20].  $\sigma_c$  and  $m_i$  can be determined by conventional triaxial tests. The parameters of USC are determined by true triaxial tests. Therefore, the difficulty level of the method for determining the parameters among these three criteria is similar to the types of rock.

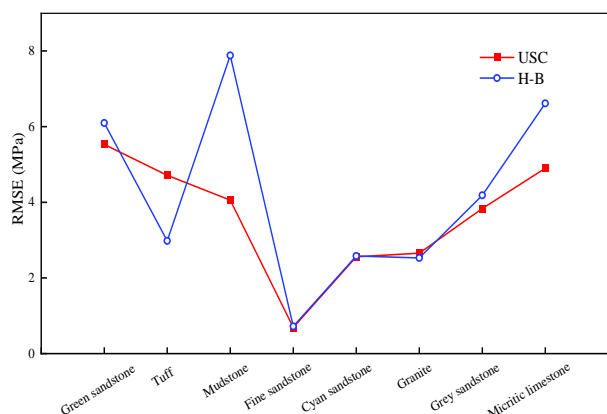


Fig. 7. RMSE of  $q$  from the USC and the H-B criterion.

The USC can unify the strength characteristics of different materials by adjusting the values of four independent parameters  $M_f, \sigma_0, n$  and  $\alpha$ . As shown in Figure 8,  $\sigma_0=0$  and  $\sigma_0 \neq 0$  in the USC represents cohesiveless and cohesive materials respectively (see Fig. 8a, c, e), while  $0 < n \leq 1$  in the USC represents frictional materials (see Fig. 8b, d, f). Different combinations of  $\sigma_0, n$  and  $\alpha$  can be used for describing the strength characteristics of some

specific materials. Note that the color of the 3D failure surface serves only for rendering purposes, providing a good visual effect without the specific meaning. The parameter value can be classified into three categories.

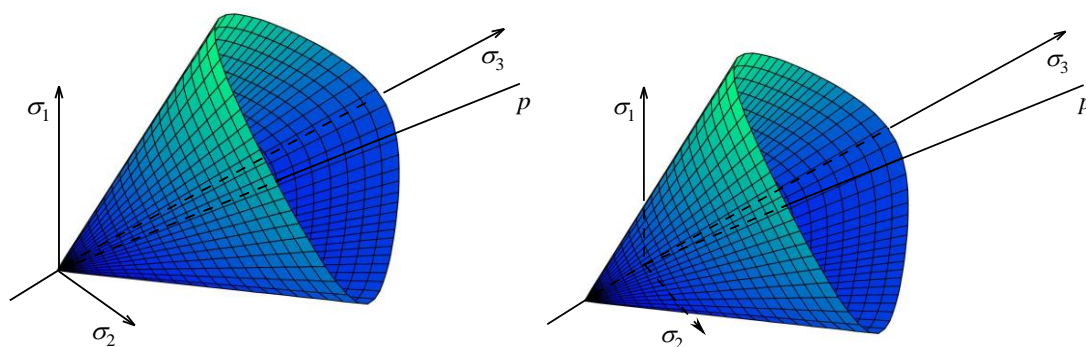
The first category for parameter value is that  $n=1, \alpha=0$  (see Fig. 8a, b). When  $\sigma_0=0$ , the USC reduces to the SMP criterion, which can be applied to sands and saturated clays (see Fig. 8a). When  $\sigma_0 \neq 0$ , cohesion is taken into account in the USC, which is identical to the extended SMP criterion [60]. In this case, the USC is appropriate for cohesive unsaturated soils and cemented sands (see Fig. 8b).

The second category for parameter value is that  $n=1, 0 < \alpha \leq 1$  (see Fig. 8c, d). The failure surface of the USC changes from curved triangle to circle with  $\alpha$  increasing. When  $\sigma_0=0$ , the USC can be used to describe the strength characteristics of sands and saturated clays (see Fig. 8c). When  $\sigma_0 \neq 0$ , the USC is appropriate for cohesive unsaturated soils and cemented sands (see Fig. 8d).

The third category for parameter value is that  $0 < n < 1, 0 < \alpha < 1$  (see Fig. 8e, f). The coupling effect of the strength on meridian plane and deviatoric plane can be taken into account. When  $\sigma_0 \neq 0$ , the USC can be applied to nonlinear cohesiveless materials, such as gravels (see Fig. 8e). When  $\sigma_0 \neq 0$ , the USC is in the general form. In this case, the material is cohesive, and the internal friction angle varies nonlinearly with hydrostatic pressure increasing (see Fig. 8f). Thus, the applicable scope of the USC can be expanded under, which means that the strength characteristics of rock and concretes can be described by the USC under as well.

In conclusion, the USC can be applied for describing the strength characteristics of soils, gravels, concretes and rocks by adjusting the value of relevant parameters.

Compared to the original H-B criterion, the GUST, and the 3D H-B criterion, the USC not only clearly reflects the shear yield and failure characteristics of rocks under three-dimensional stress condition but also facilitates the integration with the specific elastoplastic constitutive models [61-63]. There are numerous structural planes in rock mass that can affect the stability of engineering projects. To more accurately assess stability of the projects, the primary task is to accurately predict the strength of the rock mass. Although the USC has demonstrated good accuracy in predicting the strength of intact rock, it has not been proven effective in predicting rock mass strength. Therefore, in future research, the focus will be on predicting rock mass strength and establishing the corresponding elastoplastic constitutive model.



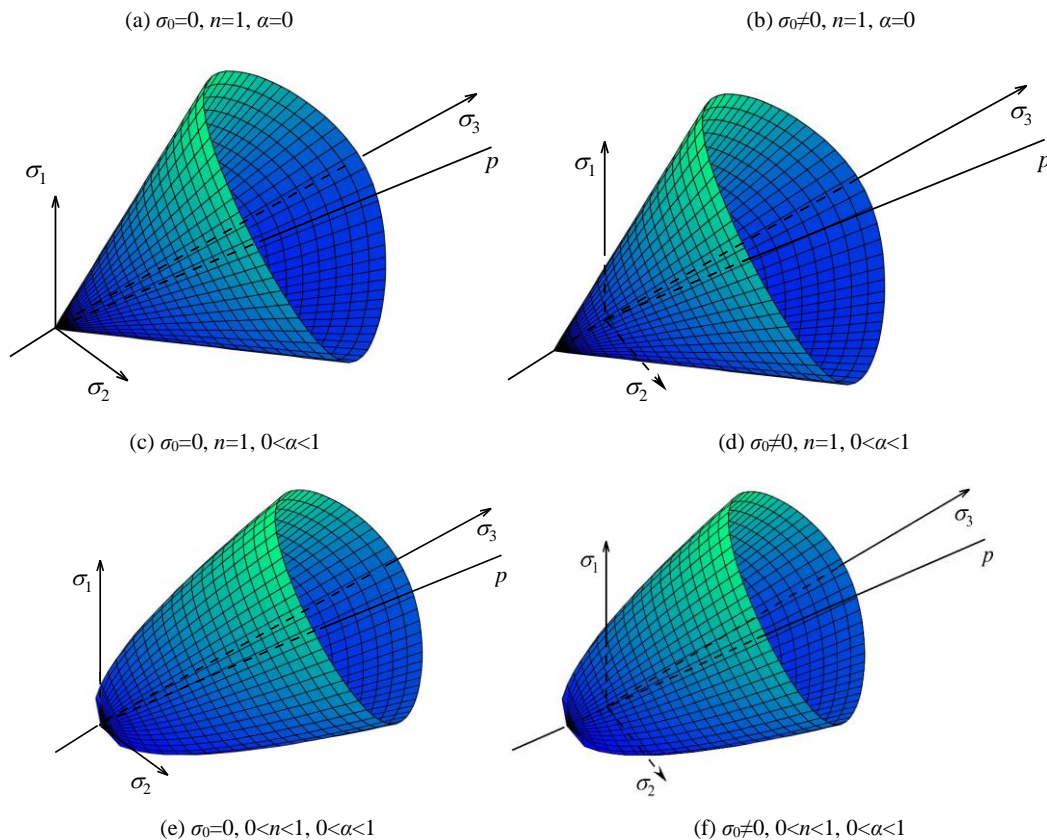


**Fig. 8.** Failure surfaces of the USC in principal stress space.

## 7. Conclusion

In this paper, three typical types of rock strength criteria are selected to fit the true triaxial experimental results of five types of rock from the reference. The pros and cons of the USC, 3D H-B, and GUST criteria are compared. Based on the conventional triaxial test results of eight types of rock, the accuracy of the original H-B criterion and the USC in predicting rock strength on meridian plane is compared. Finally, the meaning and determination method of the parameters in each criterion is discussed.

1. The USC is constructed by combining the failure functions on deviatoric and meridian planes. The USC can predict the strength of various geomaterials. The 3D H-B criterion is established in  $\beta$  stress space. The GUST introduces a weighted parameter  $\chi$  to correct the UST.

2. The predictions of strength on  $\sigma_1$ - $\sigma_2$  plane under the true triaxial test condition for five types of rock are compared among the 3D H-B, the USC and the GUST. The USC effectively reflects the influence of the intermediate principal stress on rock strength and accurately predicts rock strength under both triaxial tension and triaxial compression.

3. The predicted strength on meridian plane under the triaxial test condition for eight types of rock are compared between the original H-B criterion and the USC. The results indicate that the USC criterion is applicable to various types of rock and has a higher degree of accuracy.

4. The difficulty level of the method for determining the parameters among these three criteria is similar for various types of rock. The USC are appropriate for more types of geomaterials.

## Author contributions

Qin Yang: Writing – original draft, Validation, Investigation. Mingming He: Writing – original draft, Validation, Investigation, Data curation. Panagiotis G. Asteris: Writing – review & editing, Investigation, Funding acquisition. Qin Zhao: Writing – review & editing, Formal analysis, Data curation.

## Acknowledgments

This paper is supported by the National Natural Science Foundation of China (Grants No. 42177158 and U2368203). The authors would like to thank Prof. Yangping Yao, Prof. Dechun Lu and Prof. Jingqi Huang for their help and suggestions in preparing the manuscript.

## Conflicts of Interest

All the authors claim that the manuscript is completely original. The authors also declare no conflict of interest.

## References

- Liu JC, Li X, Xiao JJ, Xie YC, Xia KW. Three-dimensional strength criterion for rocks: A review. *Energy Reviews*. 2024; 3(4): 100102. <https://doi.org/10.1016/j.enrev.2024.100102>
- Brown ET, Hoek E. *Underground excavations in rock*. CRC Press. 1980.
- Hoek E, Brown ET. Empirical strength criterion for rock masses. *Journal of the geotechnical engineering division*. 1980; 106(9): 1013-1035.
- Lade PV. Elasto-plastic stress-strain theory for cohesionless soil with curved yield surfaces. *International journal of solids and structures*. 1977; 13(11): 1019-1035. [https://doi.org/10.1016/0020-7683\(77\)90073-7](https://doi.org/10.1016/0020-7683(77)90073-7)
- Lade PV. Modeling failure in cross-anisotropic frictional materials. *International Journal of Solids and Structures*. 2007; 44(16): 5146-5162. <https://doi.org/10.1016/j.ijsolstr.2006.12.027>
- Matsuoka H, Nakai T. Relationship among Tresca, Mises, Mohr-Coulomb and Matsuoka-Nakai failure criteria. *Soils and Foundations*. 1985; 25(4): 123-128. [https://doi.org/10.3208/sandf1972.25.4\\_123](https://doi.org/10.3208/sandf1972.25.4_123)
- Matsuoka H, Hoshikawa T, Ueno K. A general failure criterion and stress-strain relation for granular materials to metals. *Soils and Foundations*. 1990; 30(2): 119-127. [https://doi.org/10.3208/sandf1972.30.2\\_119](https://doi.org/10.3208/sandf1972.30.2_119)
- Matsuoka H, Yao YP, Sun DA. The Cam-clay models revised by the SMP criterion. *Soils and foundations* 1999; 39(1): 81-95.
- Paul B. Generalized pyramidal fracture and yield criteria. *International Journal of Solids and Structures*. 1968; 4(2): 175-196. [https://doi.org/10.1016/0020-7683\(68\)90010-3](https://doi.org/10.1016/0020-7683(68)90010-3)
- Pan XD, Hudson JA. A simplified three-dimensional Hoek-Brown yield criterion. *ISRM International Symposium*. 1988.
- Priest SD. Determination of shear strength and three-dimensional yield strength for the Hoek-Brown criterion. *Rock Mechanics and Rock Engineering*. 2005; 38: 299-327. <http://dx.doi.org/10.1007/s00603-005-0056-5>
- Zhang LY, Zhu HH. Three-dimensional Hoek-Brown strength criterion for rocks. *Journal of Geotechnical and Geoenvironmental Engineering*. 2007; 133(9): 1128-1135. [https://doi.org/10.1061/\(asce\)1090241\(2007\)133:9\(1128\)](https://doi.org/10.1061/(asce)1090241(2007)133:9(1128))
- Zhang L. A generalized three-dimensional Hoek-Brown strength criterion. *Rock mechanics and rock engineering*. 2008; 41: 893-915. <http://dx.doi.org/10.1007/s00603-008-0169-8>
- Jiang H, Wang XW, Xie YL. New strength criteria for rocks under poly-axial compression. *Canadian Geotechnical Journal*. 2011; 48(8): 1233-1245. <https://doi.org/10.1139/t11-034>
- Lee YK, Pietruszczak S, Choi BH. Failure criteria for rocks based on smooth approximations to Mohr-Coulomb and Hoek-Brown failure functions.

- International Journal of Rock Mechanics and Mining Sciences. 2012; 56: 146-160. <https://doi.org/10.1016/j.ijrmms.2012.07.032>
16. Jiang H, Xie YL. A new three-dimensional Hoek-Brown strength criterion. *Acta Mechanica Sinica*. 2012; 28(2): 393-406. <http://dx.doi.org/10.1007/s10409-012-0054-2>
  17. Zhang Q, Zhu HH, Zhang LY. Modification of a generalized three-dimensional Hoek-Brown strength criterion. *International Journal of Rock Mechanics and Mining Sciences*. 2013; 59: 80-96. <http://dx.doi.org/10.1016/j.ijrmms.2012.12.009>
  18. Jiang H, Zhao JD. A simple three-dimensional failure criterion for rocks based on the Hoek-Brown criterion. *Rock Mechanics and Rock Engineering*. 2015; 48: 1807-1819. <http://dx.doi.org/10.1007/s00603-014-0691-9>
  19. Wu SC, Zhang SH, Zhang G. Three-dimensional strength estimation of intact rocks using a modified Hoek-Brown criterion based on a new deviatoric function. *International Journal of Rock Mechanics and Mining Sciences*. 2018; 107: 181-190. <http://dx.doi.org/10.1016/j.ijrmms.2018.04.050>
  20. Huang JQ, Du XL, Ma C. Study on three-dimensional strength criterion for rocks. *Engineering Mechanics (in Chinese)*. 2018; 35(03): 30-40.
  21. Cai W, Zhu HH, Liang WH, Zhang LY. A new version of the generalized Zhang-Zhu strength criterion and a discussion on its smoothness and convexity. *Rock Mechanics and Rock Engineering*. 2021; 54: 4265-4281. <http://dx.doi.org/10.1007/s00603-021-02505-z>
  22. Li HZ, Guo T, YL Nan, Han B. A simplified three-dimensional extension of Hoek-Brown strength criterion. *Journal of Rock Mechanics and Geotechnical Engineering*. 2021; 13(3): 568-578. <http://dx.doi.org/10.1016/j.jrmge.2020.10.004>
  23. Zienkiewicz OC, Pande GN. Some useful forms of isotropic yield surface for soil and rock mechanics. *Finite Elements*. John Wiley & Sons Press. 1977.
  24. Yu MH, He LN, Song LY. Twin shear stress theory and its generalization. *Science in China, Ser. A*. 1985; 11: 1174-1183.
  25. Yu MH. Unified strength theory for geomaterials and its applications. *Chinese Journal of Geotechnical Engineering*. 1994; 16(2): 1-10.
  26. Yu MH, He LN. A new model and theory on yield and failure of materials under the complex stress state. *Mechanical Behavior of Materials VI*. Pergamon. 1992. <https://doi.org/10.1016/B978-0-08-037890-9.50389-6>
  27. Yu MH. Advances in strength theories for materials under complex stress state in the 20th century. *Applied Mechanics Review*. 2002; 55(3): 169-218. <https://doi.org/10.1115/1.1472455>
  28. Yu MH, Yu SQ. Introduction to unified strength theory. CRC Press. 2019.
  29. Li HZ, Xu JT, Zhang ZL, Song L. A generalized unified strength theory for rocks. *Rock Mechanics and Rock Engineering*. 2023; 56(11): 7759-7776. <http://dx.doi.org/10.1007/s00603-023-03471-4>
  30. Yao YP, Lu DC, Zhou AN, Zou B. Generalized non-linear strength theory and transformed stress space. *Science in China (Series E: Technological Sciences)*. 2004; 47(6): 691-709. <http://dx.doi.org/10.1360/04ye0199>
  31. Yao YP, Hu J, Zhou AN, Luo T, Wang ND. Unified strength criterion for soils, gravels, rocks, and concretes. *Acta Geotechnica*. 2015; 10: 749-759. <http://dx.doi.org/10.1007/s11440-015-0404-x>
  32. Yao YP, Zhou AN, Lu DC. Extended transformed stress space for geomaterials and its application. *Journal of engineering mechanics*. 2007; 133(10): 1115-1123. <http://dx.doi.org/10.1061/ASCE0733-93992007133:101115>
  33. Yao YP, Tang KS. Isotropically transformed stress method for the anisotropy of soils. *Chinese Journal of Theoretical and Applied Mechanics*. 2022; 54(6): 1651-1659. <http://dx.doi.org/10.6052/0459-1879-21-651>
  34. Mogi K. Effect of the intermediate principal stress on rock failure. *Journal of Geophysical Research*. 1967; 72(20): 5117-5131.
  35. Mogi K. Fracture and flow of rocks under high triaxial compression. *Journal of Geophysical Research*. 1971; 76(5): 1255-1269.
  36. Mogi K. Effect of the triaxial stress system on the failure of dolomite and limestone. *Tectonophysics*. 1971; 11(2): 111-127. [https://doi.org/10.1016/0040-1951\(71\)90059-X](https://doi.org/10.1016/0040-1951(71)90059-X)
  37. Mogi K. *Experimental rock mechanics*. CRC Press. 2006.
  38. Takahashi M, Koide H. Effect of the intermediate principal stress on strength and deformation behavior of sedimentary rocks at the depth shallower than 2000 m. *ISRM international symposium*. 1989.
  39. Chang CD, Haimson B. True triaxial strength and deformability of the German Continental Deep Drilling Program (KTB) deep hole amphibolite. *Journal of Geophysical Research: Solid Earth*. 2000; 105(B8): 18999-19013. <https://doi.org/10.1029/2000JB900184>
  40. Haimson B, Rudnicki JW. The effect of the intermediate principal stress on fault formation and fault angle in siltstone. *Journal of Structural Geology*. 2010; 32(11): 1701-1711. <https://doi.org/10.1016/j.jsg.2009.08.017>
  41. Feng XT, Zhang XW, Kong R, Wang G. A novel Mogi type true triaxial testing apparatus and its use to obtain complete stress-strain curves of hard rocks. *Rock Mechanics and Rock Engineering*. 2016; 49: 1649-1662. <http://dx.doi.org/10.1007/s00603-015-0875-y>
  42. Feng XT, Kong R, Zhang XW, Yang CX. Experimental study of failure differences in hard rock under true triaxial compression. *Rock Mechanics and Rock Engineering*. 2019; 52: 2109-2122. <http://dx.doi.org/10.1007/s00603-018-1700-1>
  43. Feng XT, Tian M, Yang CX, He BG. A testing system to understand rock fracturing processes induced by different dynamic disturbances under true triaxial compression. *Journal of Rock Mechanics and Geotechnical Engineering*. 2023; 15(1): 102-118. <https://doi.org/10.1016/j.jrmge.2022.02.002>
  44. Du K, Yang C, Su R, Tao M. Failure properties of cubic granite, marble, and sandstone specimens under true triaxial stress. *International Journal of Rock Mechanics and Mining Sciences*. 2020; 130: 104309. <https://doi.org/10.1016/j.ijrmms.2020.104309> [Get rights and content](#)
  45. Zhu C, Karakus M, He MC, Meng Q. Volumetric deformation and damage evolution of Tibet interbedded skarn under multistage constant-amplitude-cyclic loading. *International Journal of Rock Mechanics and Mining Sciences*. 2022; 152: 105066. <https://doi.org/10.1016/j.ijrmms.2022.105066>
  46. Yao YP, Sun DA. Application of Lade's criterion to Cam-clay model. *Journal of engineering mechanics*. 2000; 126(1): 112-119.
  47. Kim M, Lade PV. Modelling rock strength in three dimensions. *International Journal of Rock Mechanics and Mining Sciences & Geomechanics Abstracts*. 1984; 21(1): 21-33. [https://doi.org/10.1016/0148-9062\(84\)90006-8](https://doi.org/10.1016/0148-9062(84)90006-8)
  48. Liu JC, Li X, Xu Y, Xia K. A three-dimensional nonlinear strength criterion for rocks considering both brittle and ductile domains. *Rock Mechanics and Rock Engineering*. 2024; 57: 5863-5881. <http://dx.doi.org/10.1007/s00603-024-03823-8>
  49. Kármán T. Festigkeitsversuche unter allseitigem Druck. *Zeitschrift Verein Deutscher Ingenieure*. 1911; 55: 1749-57.
  50. Zheng GQ, Tang YH, Zhang Y, Gao YH. Study on failure difference of hard rock based on a comparison between the conventional triaxial test and true triaxial test. *Frontiers in Earth Science*. 2022; 10: 923611. <https://doi.org/10.3389/feart.2022.923611>
  51. Xing XL, Li LT, Fu YK. Determination of the related strength parameters of unsaturated loess with conventional triaxial test. *Environmental Earth Sciences*. 2016; 75: 1-11. <http://dx.doi.org/10.1007/s12665-015-4797-5>
  52. Xie SJ, Lin H, Chen YF, Wang YX. A new nonlinear empirical strength criterion for rocks under conventional triaxial compression. *Journal of Central South University*. 2021; 28(5): 1448-1458. <http://dx.doi.org/10.1007/s11771-021-4708-8>
  53. Li XF, Ma ZG. A novel method for imitating true-triaxial stress path with conventional triaxial apparatus. *Geomechanics and Geophysics for Geo-Energy and Geo-Resources*. 2024; 10: 68. <http://dx.doi.org/10.1007/s40948-024-00781-x>
  54. Mogi K. Effect of the triaxial stress system on rock failure. *Rock Mechanics in Japan*. 1970; 1: 53-55.
  55. Lu J, Yin GZ, Zhang DM, Gao H. True triaxial strength and failure characteristics of cubic coal and sandstone under different loading paths. *International Journal of Rock Mechanics and Mining Sciences*. 2020; 135: 104439. <https://doi.org/10.1016/j.ijrmms.2020.104439>
  56. Vachaparampil A, Ghassemi A. Failure characteristics of three shales under true-triaxial compression. *International Journal of Rock Mechanics and Mining Sciences*. 2017; 100: 151-159. <https://doi.org/10.1016/j.ijrmms.2017.10.018>
  57. Feng XT, Kong R, Zhang XW, Yang CX. Experimental Study of Failure Differences in Hard Rock Under True Triaxial Compression. *Rock Mechanics and Rock Engineering*. 2019; 52(7): 2109-2122. <https://doi.org/10.1016/j.jrmms.2017.10.018>
  58. Li XB, Du K, Li DY. True triaxial strength and failure modes of cubic rock specimens with unloading the minor principal stress. *Rock Mechanics and Rock Engineering*. 2015; 48: 2185-2196. <https://doi.org/10.1007/s00603-014-0701-y>
  59. Du XL, Ma C, Lu DC. Nonlinear unified strength model of geomaterials. *Chinese Journal of Theoretical and Applied Mechanics*. 2014; 46(03): 389-397. <https://doi.org/10.6052/0459-1879-13-312>
  60. Matsuoka H, Sun DA. Extension of spatially mobilized plane (SMP) to frictional and cohesive materials and its application to cemented sands. *Soils and foundations*. 1995; 35(4): 63-72. <https://doi.org/10.3208/sandf.35.463>
  61. Yao YP, Wang ND. Transformed stress method for generalizing soil constitutive models. *Journal of Engineering Mechanics*. 2014; 140(3): 614-629.
  62. Luo T, Tian XG, Yao YP, Cui WJ. Three-dimensional asymptotic state criterion for soils. *Chinese Journal of Geotechnical Engineering*. 2011; 33(5): 792-796.
  63. Yao YP, Yamamoto H, Wang ND. Constitutive model considering sand crushing. *Soils and foundations*. 2008; 48(4): 603-608. <https://doi.org/10.3208/sandf.48.603>